

Ruchi Gupta^{1,3*}, Mayank Agarwal², Vinay Pratap Singh³

¹Pranveer Singh Institute of Technology, Kanpur India - 209305

²Institute of Engineering and Technology, Dr. RML Avadh University, Ayodhya India – 224001

³Harcourt Butler Technical University, Kanpur India – 208010

*Corresponding author: E-mail: ruchigupta3102@gmail.com

Received (Otrzymano) 25.10.2021

HA-ZnO-Fe₃O₄ COMPOSITE MANUFACTURED BY WET POWDER METALLURGY PROCESS FOR IMPLANT APPLICATIONS

A hydroxyapatite (HA) based biocompatible and bioactive composite is an appropriate choice for bio-implants. This experimental work presents the influence of ZnO and Fe₃O₄ on the microstructure of HA-ZnO-Fe₃O₄ composites synthesized by the wet powder metallurgy process. These composites were characterized using SEM, energy-dispersive X-ray spectroscopy (EDS), and XRD. The obtained results showed the effect of the addition of Fe₃O₄ on the interface formation, which is exhibited by interconnected pores and sintered neck in the micrographs. The observed porosity helps to enhance the required osseointegration for the fixation of implants with human bones.

Keywords: bioceramics, hydroxyapatite, powder metallurgy, microstructure, density

INTRODUCTION

In some clinical applications such as orthopedic implants, dental restoratives, and other medical equipment, hydroxyapatite (HA) is considered to be an attractive bio-ceramic [1-8]. Nowadays, researchers are interested in developing new bio-ceramics with improved properties by adding metals and their oxides to HA [2]. The improvement in properties is also influenced by the manufacturing process and its associated parameters apart from the material used. Therefore, due to the consolidated effect of manufacturing and materials, it is possible to improve the properties of a composite material, which are needed for implant applications [7, 9]. Various properties such as excellent corrosion resistance, low wear rate, good osseointegration with excellent biocompatibility are required for specific applications [1-8, 10, 11]. Moreover, zinc oxide (ZnO) is one of the best anti-bacterial inorganic compounds, which is safe and suitable for various drug administration applications [12]. Fe and its compounds are also utilized as nontoxic and biocompatible material when the concentration of iron is limited. Nevertheless, the addition of iron oxide nano-particles is reported to be compatible with ZnO, which is considered as an agent for antibacterial properties [13].

This research work reports the influence of the consolidated effect of ZnO and Fe₃O₄ on HA. In addition, the effect of the wet chemical processing of HA and wet powder metallurgy process with microstructural evaluation is discussed for the synthesized HA-ZnO-Fe₃O₄ composites.

MATERIALS AND METHODS

The fabrication process of the HA-ZnO-Fe₃O₄ bio-composite is described in Figure 1. In the process, first of all, the HA powder was synthesized by wet chemical processing using calcium oxide (CaO) and orthophosphoric acid (H₃PO₄). In the process, 14.67 g of CaO powder was mixed with 1000 ml of distilled water and stirred continuously with a gradual increase in the temperature up to 80°C, which was followed by the addition of a mixture of H₃PO₄+1000 ml distilled water in the form of small and continuous droplets. Next, this mixture was cooled and ball milled (Pulverisette 7 premium line, planetary mill, Fritsch, Germany) with a ball to powder ratio (by weight) of 6:1 to prepare fine HA powder (100-200 microns). A micrograph of the HA powder is shown in Figure 1. In the next step, ZnO (> 99% pure, 60-80 microns) and Fe₃O₄ (> 99% pure, 40-60 microns) powders, provided by Ms. Central Drug House, New Delhi, India, were blended (200 rpm) with HA for 6 h in an agate jar with steel balls and acetone as the mixing medium. Afterwards, the mixed powder was compacted inside an alloy steel closed die under a pressure of 430 MPa by means of a hydraulic press. After that, the fabricated green pellets 12 mm in diameter and 12-15 mm in height were air sintered inside a muffle furnace at the temperature of 1150°C with a 3 h idle time before cooling. Inside the furnace, the heating and cooling rate was 5°C/min. In the experiment, three compositions, denoted as HZ (HA +

7.5 wt.% ZnO), HZ10F (HA + 7.5 wt.% ZnO + 10 wt.% Fe₃O₄) and HZ20F (HA + 7.5 wt.% ZnO + 20 wt.% Fe₃O₄), were used for the analysis. The density of the sintered pellets was evaluated experimentally using the Archimedes' principle considering water as the fluid. The morphological evaluation and energy dispersive X-ray spectroscopy (EDS) were conducted using a scanning electron microscope (SEM, Model JSM 6010LA, JEOL), and a PANalytical X-ray diffractometer using Cu radiation at 45 kV and 40 mA was employed as well.

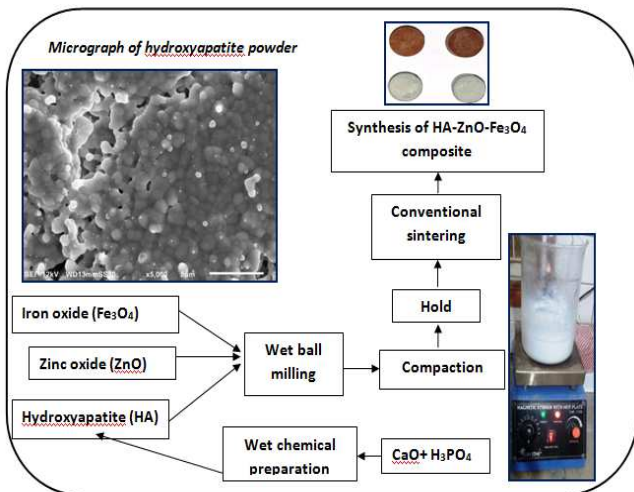


Fig. 1. Synthesis process of HA-ZnO-Fe₃O₄ composite

RESULTS AND DISCUSSION

A decrease in the density was observed with the addition of Fe₃O₄ to the HZ composites. The densities evaluated using the Archimedes' principle were 3.2, 3.1 and 2.8 g/cm³, for the HZ, HZ10F, and HZ20F compositions, respectively. The decrease may be attributed to the increase in the number of pores, which can also be observed in the micrographs below.

Figure 2a, b presents SEM micrographs revealing the microstructures of the HZ compositions at lower and higher magnifications, respectively. Dense spherical grains with distinct boundaries were found in the microstructure (marked by red boundary in Figure 2a). High densification can be seen in the micrographs and it aptly correlates with the 98% densification found experimentally using the Archimedes' principle [8]. The high level of densification is attributed to the high sintering temperature, but with the presence of some unpredicted pores, as shown in Figure 2b [10].

Figure 2c shows the XRD patterns of the sintered samples for all three compositions. The diffraction patterns of the samples were matched with the corresponding standard diffraction patterns from the ICDD database. The high-intensity characteristic peaks of the HA phase are evident. The low-intensity peak of ZnO found at the 2θ value of 36.44° is probably due to its lower concentration. Fe₃O₄ peaks were found at the 2θ values of 30.15°, 35.50°, 43.00°, 56.87°, and 62.36°

in the HZ10F and HZ20F compositions. The intensity of the Fe₃O₄ peaks was found to rise with its increase in concentration from 10 to 20 wt.%, while the intensity of the HA peaks was found to decline with the increase in Fe₃O₄ concentration [8]. The absence of any other significant phases indicates that no reaction took place among the three constituents, i.e. HA, ZnO, and Fe₃O₄, thus assuring their chemical stability [9].

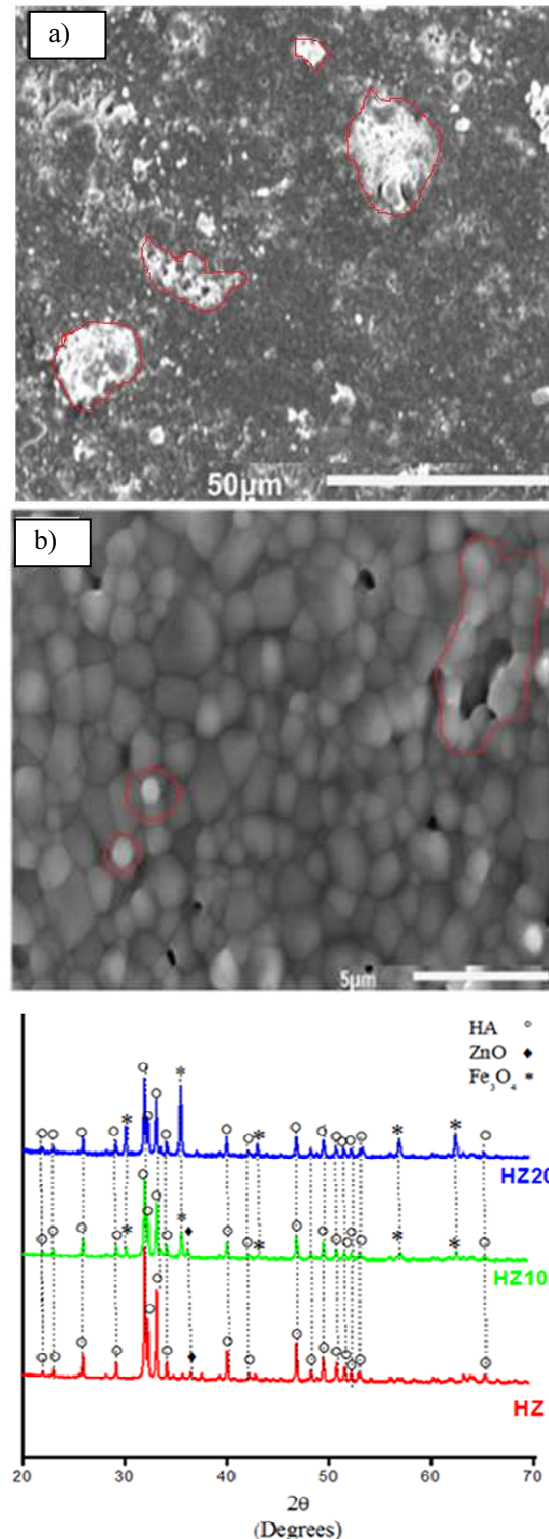


Fig. 2. Microstructure of HZ (a), ZnO particulates in HZ composite (b), XRD patterns for HZ, HZ10F and HZ20F composites (c)

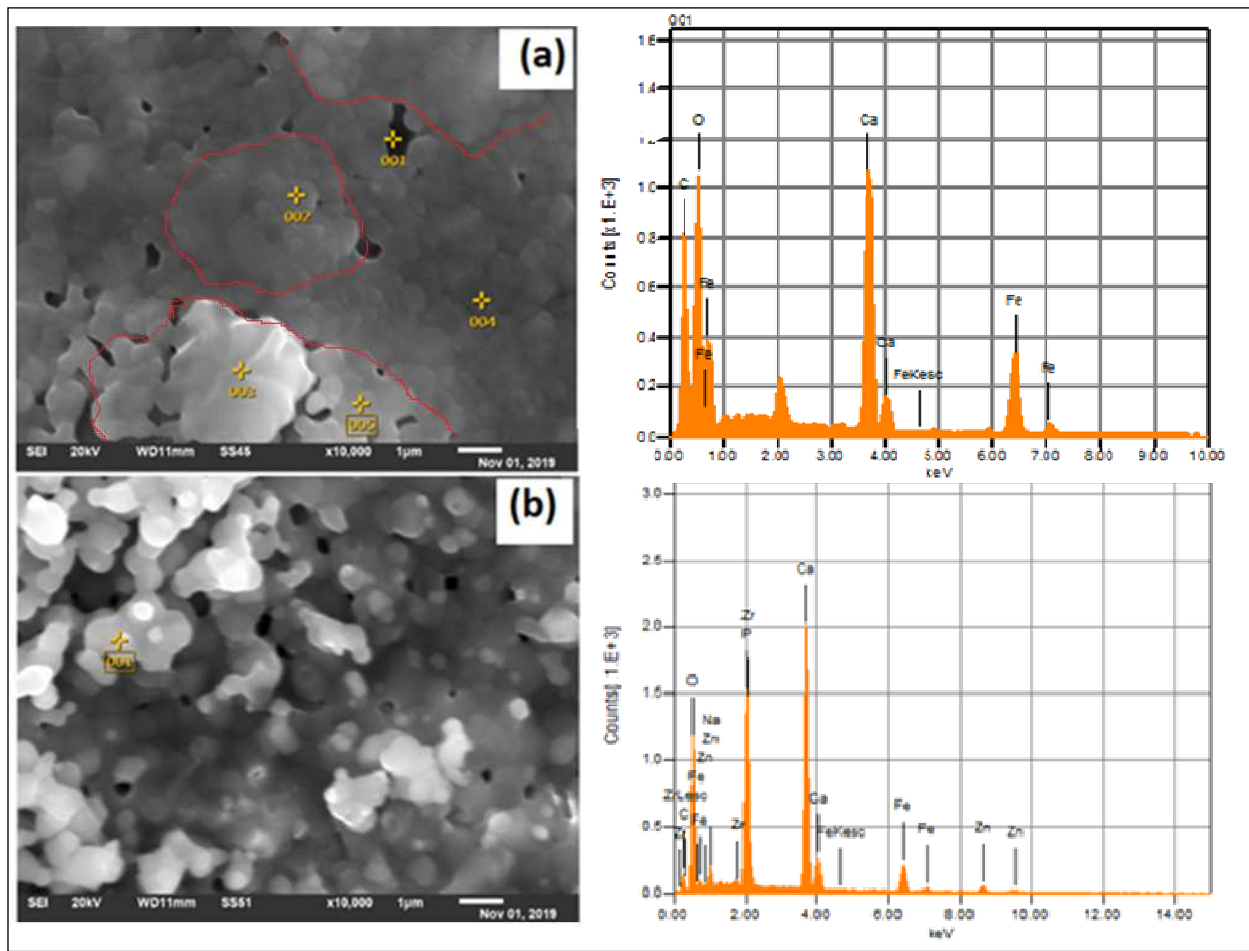


Fig. 3. EDX mapping of HA-ZnO-Fe₃O₄ composite: a) HZ10F, b) HZ20F

Figure 3a,b shows the microstructures and EDS spectra of the HZ10F and HZ20F pellets, respectively. Diffused grain boundaries and agglomerated grains are observed in both the compositions; the diffusion increased with the rise in the proportion of Fe₃O₄, which also increased the number of pores [2, 8]. The microstructure mostly consists of small pores, but some pores are interconnected; hence, they resulted in the formation of large pores [2, 12, 14]. The formation of pores may be due to the different diffusion rates of HA, ZnO, and Fe₃O₄. High porosity results in lower mechanical strength, but on other hand, it helps in the fixation of an implant with the bone.

The elemental composition obtained by EDS verifies the presence of ZnO and Fe₃O₄ in HA composites. No significant amounts of other elements can be seen in the spectra. An increase in the concentration of Fe₃O₄ in Figure 3b can also be observed in the micrographs as a greater distribution of bright white particles among the greyish particles of HA [8]. These particles are co-related with the formation of interfaces in the EDS mapped area (Fig. 3a).

According to the EDS mapping shown in Figure 3, the influence of the processing parameters and the effect of the added reinforcement can be identified by the individual elemental peaks of Zn, Fe, and Ca. Most

of these peaks confirm the dispersion of ZnO in HA, which is obvious and well predicted. This impact of the reinforcement is again related to the distribution of the reinforcement particulates and it can be concluded that an increase in the number of reinforcement particles significantly affects the dispersion, which leads to a reduction in the gaps between the solidified molecular particulates, as can be identified in Figure 4a and b.

Moreover, this dispersion is directly governed by the generated micro-sized bio-interfaces during the process as a result of an effective change in the density of the fabricated composite [9]. As the amount of reinforcement increases, the density of the composite decreases, which results in the formation of pores inside the microstructure of the fabricated composite and further affects the intermolecular gap [9, 14]. An expansion of the formed phases during processing might be the reason for the bursting of HA grains, also leads to a drop in temperature, and thus creates some bio-interfaces (marked with red box) as well as some micropores. Furthermore, this effect is observed in Figure 4, in which some interfaces, white in color are observed in the form of some agglomerated granules in the HA, which is lower for HZ10F (Fig. 4a) in comparison to HZ20F (Fig. 4b).

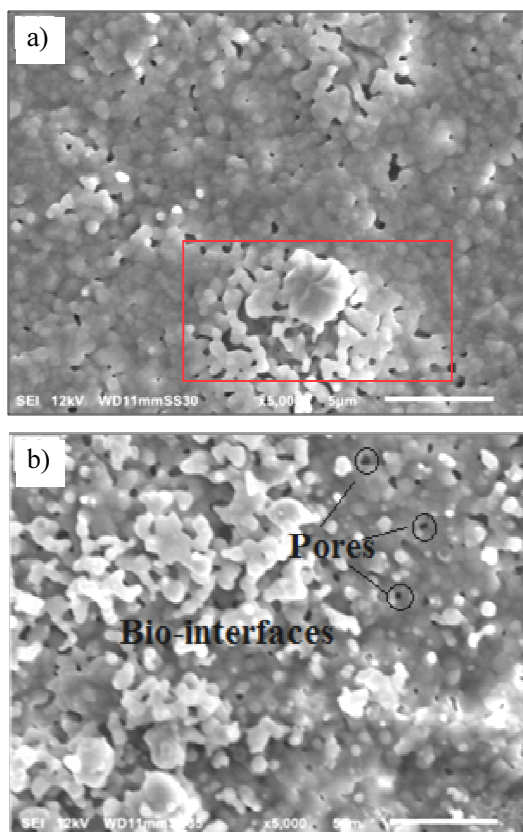


Fig. 4. Micrographs of HA-ZnO-Fe₃O₄ composite: a) HZ10F, b) HZ20F

CONCLUSIONS

Microstructural investigations were performed by SEM-EDS and XRD. The obtained micrographs and diffraction patterns were studied for all three compositions of the HA-ZnO-Fe₃O₄ composite. Dense grains with distinct grain boundaries were found in the HZ composite. The addition of Fe₃O₄ introduced porosity in the HA-ZnO composite and it grew with the increase in the weight percentage of Fe₃O₄. Interconnected pores and sintered necks were also observed in the micrographs of HZ10F and HZ20F. Porosity lowers the mechanical strength of implants but enhances the osseointegration required for the fixation of implants with human bone.

Acknowledgements

The authors would like to thank the Biomaterial Laboratory, Department of Materials Science and Engineering, IIT Kanpur, for their kind support in performing experimental work. The authors also acknowledge the Microscopy and X-Ray Diffraction facility at the Advanced Center for Materials Science, IIT Kanpur.

REFERENCES

- [1] Qi J., Xiao J., Zhang T., Zhang Y., Xiong C., Investigation of the nano-hydroxyapatite with different surface modifications on the properties of poly(lactide-co-glycolide acid)/poly(trimethylene carbonate)/nano-hydroxyapatite composites, Col. Pol. Sci. 2021, 299, 623-635, DOI: 10.1007/s00396-020-04783-5.
- [2] Kumar C.S., Dhanaraj K., Vimalathithan R.M., Ilaiyaraja P., Suresh G., Hydroxyapatite for bone related applications derived from sea shell waste by simple precipitation method, J. of Asian Cer. Soc. 2020, 8, 2, 416-429, DOI: 10.1080/21870764.2020.1749373.
- [3] Verma N., Zafar S., Talha M., Application of microwave energy for rapid fabrication of nano-hydroxyapatite reinforced polycaprolactone composite foam, Manuf. Lett. 2020, 23, 9-13, DOI: 10.1016/j.mfglet.2019.11.006.
- [4] Mushtaq A., Zhao R., Luo D., Dempsey E., Wang X., Iqbal M.Z., Kong X., Magnetic hydroxyapatite nanocomposites: the advances from synthesis to biomedical applications, Mat. Des. 2021, 197, 109269, DOI: 10.1016/j.matdes.2020.109269.
- [5] Rajesh R., Ravichandran Y.D., Raj N.A.N., Senthilkumar N., Development of a biodegradable composite (hydroxyapatite-chitosan-coir pith) as a packing material, Polymer-Plastics Tech. Eng. 2014, 53, 11, 1105-1110, DOI: 10.1080/03602559.2014.886075.
- [6] Bhatt A., Sakai K., Madhyastha R., Murayama M., Madhyastha H., Rath S.N., Biosynthesis and characterization of nano magnetic hydroxyapatite (nMHAp): An accelerated approach using simulated body fluid for biomedical application, Cer. Inter. 2020, 46, 17, 27866-27876, DOI: 10.1016/j.ceramint.2020.07.285.
- [7] Torgbo S., Sukyai P., Fabrication of microporous bacterial cellulose embedded with magnetite and hydroxyapatite nanocomposite scaffold for bone tissue engineering, Mater. Chem. Phys. 2019, 237, 121868, DOI: 10.1016/j.matchemphys.2019.121868.
- [8] Gupta R., Singh V.P., Determination of mechanical properties and physical characterization of HA-ZnO-Fe₃O₄ composites for implant applications, J. of Mater. Eng and Perf. 2021, 30, 955-963, DOI: 10.1007/s11665-020-05385-6.
- [9] Balázs C., Bishop A., Yang J.H.C., Balázs K., Wéber F., Gouma P., Biopolymer-hydroxyapatite scaffolds for advanced prosthetics, Comp. Inter. 2009, 16, 2-3, 191-200, DOI: 10.1163/156855408X402902.
- [10] Wojteczko A., Wojteczko K., Strzelecka M., Nam T., Jach K., Rosiński M., Bučko M.M., Pędzich Z., The influence of sintering technique on microstructure and properties of ZrO₂/Al₂O₃ composite, Composites Theory and Practice 2019, 19, 4, 157-160.
- [11] Khader A., Arinze T.L., Biodegradable zinc oxide composite scaffolds promote osteochondral differentiation of mesenchymal stem cells, Biotech. Bioeng. 2020, 117, 194-209, DOI: 10.1002/bit.27173.
- [12] Maleki-Ghaleh H., Aghaie E., Nadernezhad A., Zargarzadeh M., Khakzad A., Shakeri M.S., Beygi Khosrowshahi Y., Siadati M.H., Influence of Fe₃O₄ nanoparticles in hydroxyapatite scaffolds on proliferation of primary human fibroblast cells, J. of Mater. Eng and Perf. 2016, 25 2331-2339, DOI: 10.1007/s11665-016-2086-4.
- [13] Kuda O., Pinchuk N., Bykov O., Tomila T., Olifan O., Golovkova M., Development and characterization of sr-containing glass-ceramic composites based on biogenic hydroxyapatite, Nanoscale Res. Lett. 2018, 13, 155, DOI: 10.1186/s11671-018-2550-1.
- [14] Baji A., Wong S., Srivatsan T.S., Njus G.O., Mathur G., Processing methodologies for polycaprolactone-hydroxyapatite composites: A review, Mat. Manu. Proc. 2006, 21, 2, 211-218, DOI: 10.1081/AMP-200068681.